Energy Efficiency and Spectral Efficiency Tradeoff in Type-I ARQ Systems

Jingxian Wu, *Member, IEEE*, Gang Wang, *Student Member, IEEE*, and Yahong Rosa Zheng, *Senior Member, IEEE*

***Abstract*—The optimum energy efficient and spectral efficient designs for type-I automatic-repeat-request (ARQ) systems in Rayleigh flat fading channels are studied in this paper. Three optimum designs are considered: the first scheme maximizes the energy efficiency (EE), or equivalently, minimizes the total energy per information bit without considering the spectral efficiency (SE); the second scheme minimizes a new metric, the energy per information bit normalized by the SE; and the third scheme maximizes the EE under the constraint of a minimum SE. For given physical and link layer parameters, such as hardware power consumption, coding rate, modulation, bit rate, number of overhead bits, and communication distance, the three schemes are optimized with respect to the average transmission energy and the number of information bits per frame. The fundamental EE-SE tradeoff curve is analytically identified via the optimization of the third scheme, and it is shown that the optimum EE is quansiconcave in SE in a type-I ARQ system. The optimum solutions to the first two schemes are special operating points on the EE-SE tradeoff curve. Computer simulation results verify the analytical solutions.**

***Index Terms*—Cross-layer design, ARQ, energy efficiency, spectral efficiency, green communications.**

I. Introduction

ENERGY efficiency (EE) and spectral efficiency (SE) are two essential design metrics for wireless communication systems. Energy efficient communication reduces energy consumption and extends the battery life of wireless terminals [1]. On the other hand, spectral efficient communication aims at supporting more simultaneous users or achieving a higher data rate with the scarce spectrum resource. However, EE and SE are often conflicting goals, featuring one of the most fundamental tradeoffs in communication system designs. Therefore, it is imperative to understand the tradeoff and develop optimum schemes that are efficient in terms of both energy and spectrum.

Manuscript received April 10, 2012; revised October 31, 2012 and Feb. 17, 2013. The work of J. Wu and G. Wang was supported in part by U.S. National Science Foundation under Grant ECCS-1202075. The work of Y.R. Zheng was supported in part by the U.S. National Science Foundation under Grant ECCS-0846486. Part of the material in this paper has been presented at the IEEE Global Telecommunication Conference, Anaheim, CA, 2012.

J. Wu and G. Wang are with the Department of Electrical Engineering, University of Arkansas, Fayetteville, AR 72701, USA (e-mail: wuj@uark.edu; wangg@email.uark.edu).

Y.R. Zheng is with the Department of Electrical and Computer Engineering, Missouri University of Science and Technology, Rolla, MO 65409, USA (e-mail: zhengyr@mst.edu).

Digital Object Identifier 10.1109/JSAC.2014.141215.

A large number of works are devoted to the development of energy efficient communication systems [2]–[7]. In the physical (PHY) layer, energy efficient communication techniques are mainly developed through coding, modulation, and signal processing techniques [2] and [3]. In the medium access control (MAC) layer, the energy consumption can be reduced in a number of ways, such as decreasing the transmission duty cycle [4], or reducing collisions via careful scheduling [5], etc. A PHY/MAC cross-layer design framework is considered in [6] for hybrid automatic-repeat-request (HARQ) in fading channels, where the optimum power assignment is studied to reduce the total average power consumption. Similarly, [7] investigates the power control of incremental redundancy HARQ with constraints on packet drop probability and peak power. However, the optimization in [6] and [7] are performed under the constraint of a targeted outage probability without considering the effects of practical system parameters such as overhead, modulation, data rate, bit error rate (BER), and practical codes, etc.

Recently, the research interests have been shifted to the EE-SE tradeoff [8]–[11]. The information theoretic study in [8] identifies the fundamental tradeoff between EE and SE in the wideband and low energy regime, and it is shown that SE is a decreasing function in EE for various channels. Incorporating more practical parameters, such as circuit power and orthogonal frequency division multiple access (OFDMA), Xiong et. al. discovered that the maximum EE is strictly quasiconcave in SE if there are sufficiently many subcarriers in a downlink OFDMA system [9]. A similar result is presented in [10], where it was shown that EE and SE can increase simultaneously for a band unlimited system under a rate constraint, and EE is a decreasing function in SE when the bandwidth is limited. In [11], the throughput of an incremental HARQ system is maximized under a power constraint with partial channel state information obtained through feedback. All works use the Shannon channel capacity to measure data rate without considering practical operations such as modulation, channel coding, or frame overhead, etc.

In this paper, we study the optimum energy- and spectral-efficient designs of type-I ARQ systems, where a package is retransmitted if it cannot be recovered at the receiver. Although many varieties of ARQ and HARQ systems exist that offer different tradeoffs between the performance and complexity [6], [7], [11]–[13], type-I ARQ has a wide range of applications due to its simplicity that is especially important for low cost and low energy communication systems. Three

optimization schemes are considered for type-I ARQ in flat fading channels: the first scheme aims to minimize the energy per information bit $E_{\rm t}$, which is the energy required to successfully deliver one information bit from a transmitter to a receiver; the second scheme minimizes the normalized energy per information bit $E_{\rm m} = \frac{E_{\rm t}}{\eta_{\rm s}}$, where $\eta_{\rm s}$ is the SE in bps/Hz; and the third scheme minimizes $E_{\rm t}$ under the constraint of a minimum SE, $\eta_{\rm s} \geq \eta_{\rm th}$, with $\eta_{\rm th}$ being a constant threshold. The first scheme minimizes the overall energy consumption at the cost of the SE. The second metric $E_{\rm m}$ can be minimized by either reducing $E_{\rm t}$ or increasing $\eta_{\rm s}$, thus providing one possible tradeoff between EE and SE. The third optimization scheme allows us to flexibly adjust the EE-SE tradeoff based on specific system requirements, and it includes the $E_{\rm t}$ or $E_{\rm m}$ minimization as special cases.

The optimum designs are performed by jointly optimizing the transmission energy in the PHY layer and the frame length in the MAC layer. The system designs incorporate a large number of practical system parameters, such as the efficiency of the power amplifier, the power consumption of digital hardware, data rate, coding and modulation, frame length and protocol overhead, frame error rate (FER), and frame retransmission, etc. To quantify the impacts of transmission energy and frame length, a new log-domain threshold approximation to FER in Rayleigh fading channels is proposed, which enables explicit analytical solutions to the three optimization schemes.

Another important contribution of this paper is that the fundamental EE-SE tradeoff for type-I ARQ systems are identified through theoretical analysis of the third optimization scheme. The result corroborates that the minimum energy per information bit, which is inversely proportional to the EE, is quasiconvex in the SE, or equivalently, the EE is quasiconcave in the SE. This result agrees with the EE-SE tradeoff relationship presented in [9] for the downlink OFDMA system. Due to the quasiconvexity, the $E_{\rm t}$–$\eta_{\rm s}$ curve can be divided into two regions, one with a negative slope and the other one with a positive slope. The operation parameters corresponding to the negative slope region of the $E_{\rm t}$–$\eta_{\rm s}$ curve are not desirable for practical operations, because there always exist parameters that can outperform any point in this region in terms of both EE and SE. The non-negative slope region of the $E_{\rm t}$–$\eta_{\rm s}$ curve reveals the fundamental EE-SE tradeoff in ARQ systems. It provides a general optimization framework that enables us to obtain optimum system designs by flexibly adjusting the EE-SE tradeoffs based on the various requirements of practical systems.

II. System Model

A. EE and SE of ARQ-I Systems

Consider a transmitter and a receiver separated by a distance d. The information bits at the transmitter are divided into frames. Each frame has L uncoded information bits and L_0 overhead bits. The information and overhead bits are encoded with a rate-r channel code. For a system employing M-ary quadrature amplitude modulation (MQAM), the number of symbols in each frame is $L_{\rm s} = \frac{L+L_0}{r\log_2 M}$, where L is chosen such that $L_{\rm s}$ is an integer.

The signal is transmitted through a flat Rayleigh fading channel and the discrete-time samples at the receiver can be represented as

$$y_i = h \cdot \sqrt{E_{\rm r}} x_i + z_i, \qquad i = 1, 2, \cdots, L_{\rm s}, \tag{1}$$

where i is the symbol index in the frame, $x_i \in \mathcal{S}$ is the modulated symbol with unit energy, with $\mathcal{S}$ being the modulation constellation set of cardinality $M = |\mathcal{S}|$, $E_{\rm r}$ is the average energy of the symbol observed at the receiver, and y_i, h, and z_i are the received sample, the fading channel coefficient, and additive white Gaussian noise (AWGN) with one-sided power spectral density N_0, respectively. It is assumed that the system undergoes quasi-static Rayleigh fading, such that the fading coefficient is constant within one frame, but changes from frame to frame.

Let $E_{\rm b}$ denote the average energy per uncoded bit, then the average $E_{\rm b}/N_0$ at the receiver is

$$\gamma_{\rm b} \triangleq \frac{E_{\rm b}}{N_0} = \frac{E_{\rm r}}{rN_0 \log_2 M}. \tag{2}$$

The average transmission energy for each symbol is [2]

$$E_{\rm s} = E_{\rm r} G_d, \tag{3}$$

where $G_d = G_1 d^{\kappa} M_{\rm l}$ with κ being the path-loss exponent, G_1 being the gain factor (including path-loss and antenna gain) at unit distance, and $M_{\rm l}$ being the link margin compensating the variations in hardware process and other additive background noise or interference.

In addition to the actual transmission energy, we also consider the hardware energy per symbol in the transmitter and receiver, which can be modelled as [2],

$$E_{\rm c} = \left(\frac{\zeta_M}{\mu} - 1\right) E_{\rm s} + \frac{\beta}{R_{\rm s}}, \tag{4}$$

where $R_{\rm s}$ is the gross symbol rate, μ is the drain efficiency of the power amplifier, ζ_M is the peak-to-average power ratio (PAPR) of an M-ary modulation signal, β incorporates the effects of baseband processing in the transmitter and receiver, such as signal processing, encoding and decoding, modulation and demodulation, and it can be treated as a constant determined by the particular transceiver structure. For MQAM systems, $\zeta_M \simeq 3(\sqrt{M} - \frac{1}{\sqrt{M}} + 1)$ for $M \geq 4$ [14].

From (2), (3), and (4), the average energy required to transmit an information bit during one transmission attempt is

$$E_0 = \frac{L_{\rm s}}{L}(E_{\rm s} + E_{\rm c}) = \frac{L + L_0}{L}\gamma_{\rm b} A + B, \tag{5}$$

where $A = \frac{\zeta_M N_0 G_d}{\mu}$, and $B = \frac{\beta}{R_{\rm s}} \cdot \frac{L_{\rm s}}{L} = \frac{\beta}{R_{\rm b}}$ with $R_{\rm b}$ being the information bit rate.

Due to the effects of channel fading and noise, the receiver might not be able to successfully recover the transmitted signal. The probability that a transmitted frame cannot be recovered equals to FER, which is a function of $\gamma_{\rm b}$ at the receiver, the frame length $L_{\rm s}$, the modulation level M, and the channel code. For a system employing type-I ARQ, the receiver will send a negative acknowledgment (NACK) to the transmitter if a packet cannot be recovered, and the packet will be retransmitted. Since the retransmissions are independent, the number of retransmissions K is a geometric

random variable with the probability mass function $P_K(k) = \text{FER}^{k-1}(1-\text{FER})$. The average number of retransmissions is

$$\Lambda = \frac{1}{1-\text{FER}}. \tag{6}$$

The result in (6) is obtained by assuming no limit on the number of retransmissions, which is often used to model delay tolerant communication systems. Even though there is no retransmission limit, the average number of retransmissions Λ is usually very small in reasonable communication systems, for example, $\Lambda = 1.25$ for an FER as high as 0.25. The average number of retransmissions for systems with retransmission limits falls between $[1, \Lambda]$. Therefore, imposing a retransmission limit has a relatively small impact on the average number of retransmissions.

With the effects of retransmissions, the total average energy required to successfully deliver an information bit from the transmitter to the receiver is $E_\text{t} = \Lambda E_0$, which can be expanded by combining (5) and (6) as

$$E_\text{t} = \frac{1}{1-\text{FER}}\left(\frac{L+L_0}{L}\gamma_\text{b}A + B\right). \tag{7}$$

The metric, energy per information bit E_t, measures the EE of the ARQ system. A smaller E_t means a better EE. The value of E_t relies on a number of system parameters, including E_b/N_0 at the receiver γ_b, the number of information bits per frame L, the number of overhead bits per frame L_0, the modulation level M, the symbol rate R_s, the code rate r, and the FER that inherently depends on all the above parameters, etc. Optimizing with respect to E_t will minimize the total energy consumption, but at the cost of reduced SE.

The SE, denoted as η_s, is defined as the net data rate of the successfully transmitted information bit divided by the required bandwidth. Since L information bits are successfully transmitted in L_s symbols with Λ retransmissions, the SE is

$$\eta_\text{s} = \frac{L}{L_\text{s}\Lambda(1+\alpha)} = \frac{L}{L+L_0}\frac{\eta_M}{\Lambda}. \tag{8}$$

where $\eta_M = \frac{r\log_2 M}{1+\alpha}$ is the maximum spectrum efficiency of an M-ary modulation scheme, and α is the roll-off factor of the pulse shaping filter, which expands the bandwidth of each symbol from R_s to $(1+\alpha)R_\text{s}$. The unit of the SE is bps/Hz.

To achieve a balanced tradeoff between the EE and the SE, we define a new metric, the normalized energy per information bit, as $E_\text{m} = \frac{E_\text{t}}{\eta_\text{s}}$, which can be minimized by either reducing E_t or increasing η_s, yielding one possible EE-SE tradeoff.

Combining (7) and (8), we can express the normalized energy per information bit as

$$E_\text{m} = \frac{1}{(1-\text{FER})^2}\frac{L+L_0}{L\eta_M}\left(\frac{L+L_0}{L}\gamma_\text{b}A + B\right). \tag{9}$$

From (7) and (9), we can see that the value of γ_b has two opposite effects on E_t and E_m. On one hand, FER is a decreasing function in γ_b. Therefore, increasing γ_b will decrease the average number of retransmissions Λ, thus reduce E_t and E_m. On the other hand, E_0 is a strictly increasing function in γ_b, thus it translates a positive relationship between γ_b and E_t or E_m. A similar observation can also be obtained for the relationship between L and E_t or E_m. Therefore, it is critical to identify the optimum values of γ_b and L that can minimize E_t or E_m. The optimum system design requires the knowledge of FER, which is discussed in the next subsection.

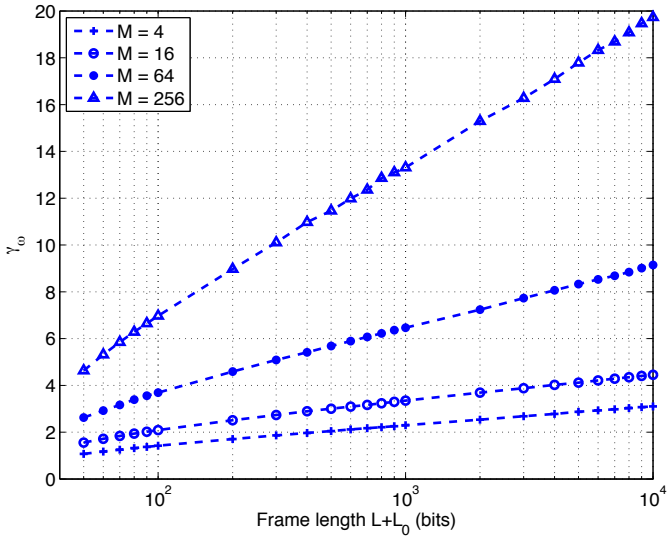

Fig. 1. Threshold γ_ω as a function of $L + L_0$ with Code 1.

B. FER with a Log-Domain Linear Threshold Approximation

In this subsection, an accurate approximation of the FER of systems operating in quasi-static Rayleigh fading is obtained with the threshold-based method originally presented in [15]. In addition, we propose a new log-domain linear approximation method for the calculation of the threshold value required for the FER approximation. The threshold-based method with the newly proposed log-domain linear approximation explicitly build a connection between the FER and the various system parameters.

The FER of a coded system in a quasi-static Rayleigh fading channel can be accurately approximated as [15]

$$\text{FER} \simeq 1 - \exp\left(-\frac{\gamma_\omega}{\gamma_\text{b}}\right), \tag{10}$$

where γ_ω is a threshold value that depends on the actual channel code, the modulation scheme, and the number of symbols per frame, etc.

Figure 1 shows γ_ω as a function of $L + L_0$ under various modulation schemes, where the values of γ_ω are estimated by matching the FER obtained through simulations with the analytical approximation in (10) using the least squares (LS) method. The channel code is the rate $r = \frac{1}{2}$ convolutional code with generator polynomial $[5, 7]_8$ and constraint length 3. It is observed from the figure that γ_ω can be approximated as a linear function of $\log(L + L_0)$, with the slope and intercept determined by different modulation schemes.

Similar linear relationships are also observed for other channel codes. Therefore, we propose to model γ_ω as

$$\gamma_\omega \simeq k_M \log(L + L_0) + b_M, \tag{11}$$

where k_M and b_M are, respectively, the slope and intercept, the values of which for several codes are listed in Table 1.

TABLE I
k_M AND b_M IN (11)

	QPSK		16QAM		64QAM	
	k_M	b_M	k_M	b_M	k_M	b_M
Uncoded	0.931	-1.223	2.327	-3.736	6.471	-11.880
Code 1	0.374	-0.310	0.523	-0.314	1.186	-1.763
Code 2	0.207	0.140	0.341	0.164	0.667	-0.130
Code 3	0.472	-0.860	1.203	-3.267	2.840	-9.348
Turbo Code	0.053	0.836	0.087	1.191	0.164	1.590

Code 1 is a rate $r = \frac{1}{2}$ convolutional code with generator polynomial $[5, 7]_8$ and constraint length 3. Code 2 is a rate $r = \frac{1}{2}$ convolutional code with generator polynomial $[171, 133]_8$ and constraint length 7. Code 3 is a rate $r = \frac{2}{3}$ convolutional code with generator polynomial $[51, 31, 13]_8$ and constraint length 3. Soft Viterbi decoders are employed for decoding the convolutional codes. The turbo code is a rate $r = \frac{1}{3}$ code with generator polynomial $[1, 5/7, 5/7]_8$ and a block interleaver. The turbo decode is performed with six iterations. It is noted that turbo code with a random interleaver might yield different results [18].

Combining (10) and (11) leads to a new approximation for the FER

$$\text{FER} \simeq 1 - (L + L_0)^{-\frac{k_M}{\gamma_\text{b}}} \exp\left(-\frac{b_M}{\gamma_\text{b}}\right). \tag{12}$$

Figure 2 compares the actual FER obtained through simulations with the analytical approximation (12) under different values of $L+L_0$ for systems with $M = 4$. The comparisons are performed for systems with various coding schemes. Excellent agreements are observed between the actual simulation results and their analytical approximations.

III. Minimizing Energy Per Information Bit

This section derives the optimum values of γ_b and L that minimize the energy per information bit E_t.

A. Optimum γ_b for minimum E_t

Before proceeding to the actual optimization, we present the following lemma about convexity of the cost function.

Lemma 1: Consider a decreasing function $f(x)$ with $f'(x) \leq 0$, and an increasing function $g(x)$ with $g'(x) \geq 0$. If both $f(x)$ and $g(x)$ are convex, then $f(x)g(x)$ is convex.

Proof: The proof is in Appendix A. ■

Since E_t is the product of the number of retransmissions Λ and the average energy in one transmission E_0 in (5), we can prove that E_t is convex in γ_b if Λ and E_0 satisfy the conditions stated in Lemma 1. The results are stated as follows.

Corollary 1: For the FER given in (12), the total energy per information bit E_t in (7) is convex in γ_b.

Proof: The proof is in Appendix B. ■

Once the convexity of E_t in γ_b is established, the optimum γ_b can be obtained through convex optimization and the result is in Proposition 1.

Proposition 1: In a quasi-static Rayleigh fading channel, if the FER is given in (12), then the optimum γ_b that minimizes

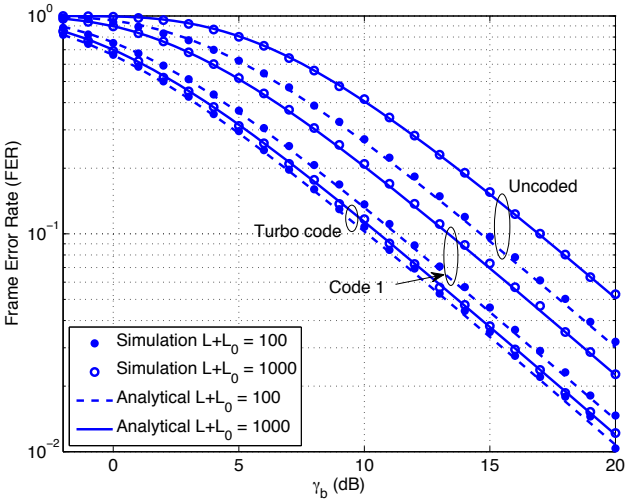

Fig. 2. Comparison of the simulated FER with the analytical approximation (12).

E_t is given by

$$\hat{\gamma}_\text{b} = \frac{1}{2}\left(\gamma_\omega + \sqrt{\gamma_\omega^2 + 4\gamma_\omega \frac{B}{A}\frac{L}{L+L_0}}\right), \tag{13}$$

where A and B are defined after (5).

Proof: The proof is in Appendix C. ■

It should be mentioned here that the optimum γ_b is the average E_b/N_0 at the receiver. Correspondingly, the optimum energy per symbol required at the transmitter is

$$\hat{E}_\text{s} = \hat{\gamma}_\text{b} N_0 G_d r \log_2 M. \tag{14}$$

B. Optimum L for minimum E_t

Similar to the results in Proposition 1, the optimum solution of L relies on the convexity of E_t. However, the direct proof of the convexity of E_t in L is quite tedious. To simplify the analysis, we show that E_t is convex in $\xi = \log(L+L_0)$. Therefore, we can solve the optimum L by indirectly minimizing E_t with respect to ξ through $\frac{\partial E_\text{t}}{\partial \xi} = 0$. It is exactly the same as solving $\frac{\partial E_\text{t}}{\partial L} = 0$ because $\frac{\partial \xi}{\partial L} = \frac{1}{L+L_0} \neq 0$.

Corollary 2: For the FER given in (12), the total energy per information bit E_t given in (7) is convex in $\xi = \log(L + L_0)$.

Proof: The proof is in Appendix D. ■

Once the convexity in ξ is established, the optimum L can be solved with result stated in Proposition 2.

Proposition 2: In a quasi-static Rayleigh fading channel, if the FER is given in (12), then the optimum L that minimizes E_t is calculated as

$$\hat{L} = \frac{\sqrt{A^2(k_M + \gamma_\text{b})^2 + 4Ak_M B} - A(k_M - \gamma_\text{b})}{2k_M(A\gamma_\text{b} + B)}\gamma_\text{b} L_0. \tag{15}$$

Proof: The proof is in Appendix E. ■

C. Joint Optimum γ_b and L for minimum E_t

The joint optimum values of γ_b and L can be obtained by solving the system of two equations defined by (13) and (15). Since both (13) and (15) are in closed forms, we can

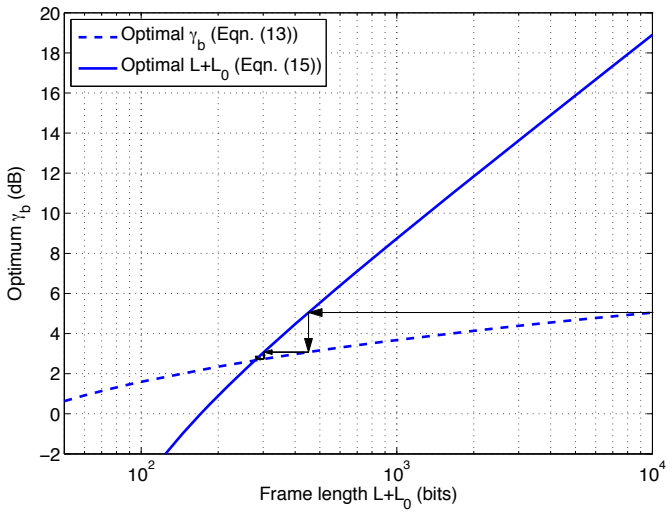

Fig. 3. Convergence of the proposed iterative method for joint optimum γ_{b} and L.

solve them by substituting (13) into (15) and then solve L numerically. This method requires the numerical solution of a nonlinear equation, and it might incur a high complexity.

Alternatively, the joint optimum values of γ_{b} and L can be calculated by iteratively invoking (13) and (15). Given an initial value L, we calculate the optimum γ_{b} using (13), the output of which is then used to update the value of L with (15). This procedure is performed iteratively and it will efficiently converge to the joint optimum value of γ_{b} and L that achieves the global minimum energy consumption.

Corollary 3: Define vector $\boldsymbol{\pi} = [\gamma_{\mathrm{b}}, L]^T$. The iterative algorithm described above will always converge to the globally optimum value $\hat{\boldsymbol{\pi}} = [\hat{\gamma}_{\mathrm{b}}, \hat{L}]^T$ that minimizes E_{t}.

Proof: The proof is in Appendix F. ∎

Figure 3 visualizes the convergence of the proposed iterative procedure by plotting (13) and (15) in the same figure. The intersection of the two curves gives the optimum values. In the figure, we used $M = 4$ and $d = 100$ m. Given the initial value $L + L_0 = 10^4$ bits, the iteration follows the trace and converges quickly to the optimum value within three iterations.

IV. Minimizing Normalized Energy Per Information Bit

This section derives the optimum system design by minimizing the normalized energy per information bit E_{m}, which can achieve a balanced tradeoff between EE and SE. To simplify notations, denote $\Delta_1 = \frac{1}{(1-\mathrm{FER})^2}$, $\Delta_2 = \frac{L+L_0}{L\eta_{_M}}\left(\frac{L+L_0}{L}\gamma_{\mathrm{b}}A + B\right)$, then $E_{\mathrm{m}} = \Delta_1\Delta_2$.

A. Optimum γ_b for minimum E_m

Following the similar procedures as in Section III, we first prove the convexity of E_{m} with respect to γ_{b}.

Corollary 4: For the FER given in (12), the normalized energy per information bit E_{m} defined in (9) is convex in γ_{b}.

Proof: The proof is in Appendix G. ∎

The optimum γ_{b} that minimizes E_{m} can be obtained by solving $\frac{\partial E_{\mathrm{m}}}{\partial \gamma_{\mathrm{b}}} = 0$, and the result is given as follows.

Proposition 3: In a quasi-static Rayleigh fading channel, if the FER is given in (12), then the optimum γ_{b} that minimizes E_{m} is

$$\check{\gamma}_{\mathrm{b}} = \gamma_\omega + \sqrt{\gamma_\omega^2 + 2\gamma_\omega \frac{B}{A}\frac{L}{L+L_0}}. \tag{16}$$

Proof: The proof is in Appendix H. ∎

Comparing the results in Propositions 1 and 3, it is clear that $\check{\gamma}_{\mathrm{b}} > \hat{\gamma}_{\mathrm{b}}$. Therefore, the system that is optimum for E_{m} requires a slightly higher energy than that optimum for E_{t}. The extra energy is used to achieve a higher spectral efficiency.

B. Optimum L for minimum E_m

Corollary 5: For the FER given in (12), the normalized energy per information bit E_{m} in (9) is convex in $\xi = \log(L + L_0)$.

Proof: The proof is in Appendix I. ∎

The following proposition states the optimum value of L that minimizes E_{m}.

Proposition 4: In a quasi-static Rayleigh fading channel, the optimum L that minimizes E_{m} is given by

$$\check{L} = \frac{2A\gamma_{\mathrm{b}} - 2Ak_{_M} + B}{4k_{_M}(A\gamma_{\mathrm{b}} + B)}\gamma_{\mathrm{b}}L_0 + \frac{\sqrt{4A^2k_{_M}^2 + 4Ak_{_M}(2A\gamma_{\mathrm{b}}+3B) + (2A\gamma_{\mathrm{b}}+B)^2}}{4k_{_M}(A\gamma_{\mathrm{b}} + B)}\gamma_{\mathrm{b}}L_0. \tag{17}$$

Proof: The proof is in Appendix J. ∎

Comparing the results in Propositions 2 and 4, we have

$$\check{L} - \hat{L} = \frac{\sqrt{D + 12Ak_MB + 4A\gamma_{\mathrm{b}}B + B^2} + B}{4k_{_M}(A\gamma_{\mathrm{b}} + B)}\gamma_{\mathrm{b}}L_0 - \frac{\sqrt{D + 16Ak_{_M}B}}{4k_{_M}(A\gamma_{\mathrm{b}} + B)}\gamma_{\mathrm{b}}L_0,$$

where $D = 4A^2(k_{_M} + \gamma_{\mathrm{b}})^2$.

From (11) and (16), we have $\gamma_{\mathrm{b}} > \gamma_\omega > k_{_M}$ if $L + L_0 > \exp\left(1 + \left|\frac{b_{_M}}{k_{_M}}\right|\right)$, which are true for all practical system configurations. Therefore, $\check{L} > \hat{L}$, which means the system that is optimum with respect to E_{m} requires a longer frame than that optimum with respect to E_{t}.

The joint optimum values of γ_{b} and L that achieve the globally minimum E_{m} can be obtained with a similar iterative method as described in Sec. III-C.

V. Energy and Spectral Efficient Designs for Type-I ARQ Systems

The metric E_{m} combines E_{t} and η_{s} in the same equation to reflect their tradeoff relationship. To gain better insights on the separate effects of E_{t} and η_{s} on the system performance, we minimize E_{t} under the constraint of the spectral efficiency η_{s} in this section. The results allow us to flexibly adjust the EE-SE tradeoff based on specific system design requirements.

The constrained optimization problem is written as

$$\begin{aligned} &\text{minimize} \quad E_{\mathrm{t}} \quad \text{with respect to } \gamma_{\mathrm{b}} > 0, L > 0 \\ &\text{subject to} \quad \eta_{\mathrm{s}} \geq \eta_{\mathrm{th}}, \end{aligned} \tag{18}$$

where η_{th} is a constant threshold.

A. Minimizing E_t under constraint $\eta_s = \eta_{th}$

We first transform (18) by setting a more restrict constraint $\eta_{\mathrm{s}} = \eta_{\mathrm{th}}$, yielding a new optimization problem

$$\begin{aligned} &\text{minimize} \quad E_{\mathrm{t}} \quad \text{with respect to } \gamma_{\mathrm{b}} > 0, L > 0 \\ &\text{subject to} \quad \eta_{\mathrm{s}} = \eta_{\mathrm{th}}. \end{aligned} \tag{19}$$

The results will help us to identify the EE-SE tradeoff and solve the original optimization problem in (18).

The Lagrangian objective function of (19) can be expressed by

$$\psi(\gamma_{\mathrm{b}}, L) = \frac{1}{1-\mathrm{FER}}\left(\frac{L+L_0}{L}\gamma_{\mathrm{b}}A + B\right) + \lambda\left[\frac{L(1-\mathrm{FER})}{L+L_0}\eta_{_M} - \eta_{\mathrm{th}}\right], \tag{20}$$

where λ is the Lagrangian multiplier.

Taking the first derivative of $\psi(\gamma_{\mathrm{b}}, L)$ with respect to λ and setting the result to zero, we have

$$\exp\left(\frac{\gamma_\omega}{\gamma_{\mathrm{b}}}\right) = \frac{L}{L+L_0}\frac{\eta_{_M}}{\eta_{\mathrm{th}}}. \tag{21}$$

The first derivatives of $\psi(\gamma_{\mathrm{b}}, L)$ with respect to γ_{b} and L are

$$\begin{aligned} \frac{\partial\psi(\gamma_{\mathrm{b}}, L)}{\partial\gamma_{\mathrm{b}}} &= \exp\left(\frac{\gamma_\omega}{\gamma_{\mathrm{b}}}\right)\frac{(-\gamma_\omega)}{\gamma_{\mathrm{b}}^2}\left(\frac{L+L_0}{L}\gamma_{\mathrm{b}}A + B\right) \\ &\quad + \exp\left(\frac{\gamma_\omega}{\gamma_{\mathrm{b}}}\right)\frac{L+L_0}{L}A \\ &\quad + \lambda\frac{L}{L+L_0}\eta_{_M}\exp\left(-\frac{\gamma_\omega}{\gamma_{\mathrm{b}}}\right)\frac{\gamma_\omega}{\gamma_{\mathrm{b}}^2}, \end{aligned} \tag{22a}$$

$$\begin{aligned} \frac{\partial\psi(\gamma_{\mathrm{b}}, L)}{\partial L} &= \exp\left(\frac{\gamma_\omega}{\gamma_{\mathrm{b}}}\right)\frac{1}{\gamma_{\mathrm{b}}}\frac{k_{_M}}{L+L_0}\left(\frac{L+L_0}{L}\gamma_{\mathrm{b}}A + B\right) \\ &\quad + \exp\left(\frac{\gamma_\omega}{\gamma_{\mathrm{b}}}\right)\gamma_{\mathrm{b}}A\frac{(-L_0)}{L^2} \\ &\quad + \lambda\eta_{_M}\left[\frac{L_0}{(L+L_0)^2}\exp\left(-\frac{\gamma_\omega}{\gamma_{\mathrm{b}}}\right)\right. \\ &\quad \left. + \frac{L}{L+L_0}\exp\left(-\frac{\gamma_\omega}{\gamma_{\mathrm{b}}}\right)\frac{(-1)}{\gamma_{\mathrm{b}}}\frac{k_{_M}}{L+L_0}\right]. \end{aligned} \tag{22b}$$

The joint optimum γ_{b} and L can be obtained by solving the equation system, $\partial\psi(\gamma_{\mathrm{b}}, L)/\partial\gamma_{\mathrm{b}} = 0$ and $\partial\psi(\gamma_{\mathrm{b}}, L)/\partial L = 0$, with the condition in (21). The result is given in Lemma 2.

Lemma 2: For an ARQ system operating in a quasi-static Rayleigh fading channel, given a constraint on the spectral efficiency $\eta_{\mathrm{s}} = \eta_{\mathrm{th}}$, the optimum values, $\tilde{\gamma}_{\mathrm{b}}$ and $\tilde{L}$ that minimize E_{t} must satisfy the following equations

$$\tilde{\gamma}_{\mathrm{b}} = \frac{1}{2}\frac{\tilde{L}}{L_0}\left(k_{_M} + \sqrt{k_{_M}^2 + 4\gamma_\omega\frac{B}{A}\frac{L_0^2}{\tilde{L}(\tilde{L}+L_0)}}\right). \tag{23}$$

and

$$\tilde{L}^{-1}(\tilde{L}+L_0)^{\frac{k_{_M}}{\gamma_{\mathrm{b}}}+1} = \frac{\eta_{_M}}{\eta_{\mathrm{th}}}\exp\left(-\frac{b_{_M}}{\tilde{\gamma}_{\mathrm{b}}}\right). \tag{24}$$

Proof: The proof is in Appendix K. ■

The optimum $\tilde{L}$ can be obtained by substituting (23) into (24) and solving for $\tilde{L}$ numerically. The optimum $\tilde{\gamma}_{\mathrm{b}}$ can then be calculated by using (23) and the optimum $\tilde{L}$.

Corollary 6: With the optimum $\tilde{\gamma}_b$ and $\tilde{L}$ obtained from Lemma 2, we conclude: 1) $\tilde{\gamma}_{\mathrm{b}}$ is a strictly increasing function in $\tilde{L}$; 2) η_{s} is a strictly increasing function in $\tilde{\gamma}_{\mathrm{b}}$; and 3) η_{s} is a strictly increasing function in $\tilde{L}$.

Proof: The proof is in Appendix L. ■

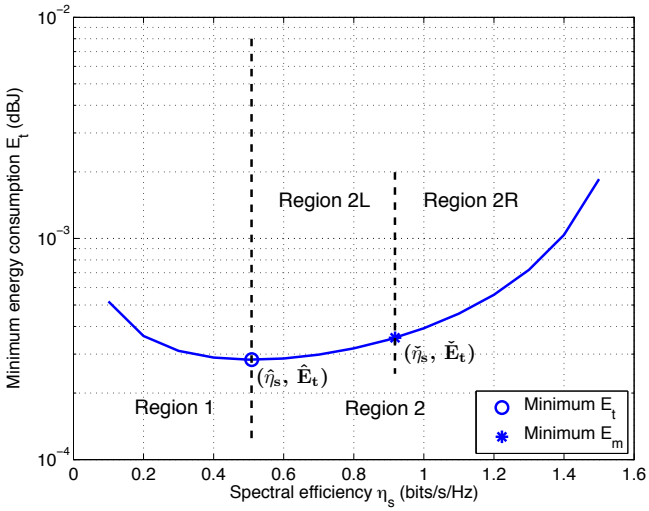

Fig. 4. Minimum energy per information bit E_{t} v.s. spectral efficiency η_{s} under the constraint of $\eta_{\mathrm{s}} = \eta_{\mathrm{th}}$. The optimum point $(\hat{\eta}_{\mathrm{s}}, \hat{E}_{\mathrm{t}})$ is obtained by minimizing E_{t}. The optimum point $(\check{\eta}_{\mathrm{s}}, \check{E}_{\mathrm{t}})$ is obtained by minimizing E_{m}.

B. EE-SE tradeoff

To illustrate the tradeoff between the energy efficiency and spectral efficiency, we plot the optimum $(\eta_{\mathrm{s}}, E_{\mathrm{t}})$ values obtained from (23) and (24) by varying the threshold $\eta_{\mathrm{s}} = \eta_{\mathrm{th}}$. The curve, denoted as the $\tilde{E}_{\mathrm{t}}(\eta_{\mathrm{s}})$ curve, is shown in Fig. 4 for the case where Code 1 in Table 1 and 16QAM modulation are used, and the maximum spectral efficiency is $\eta_{_M} = \frac{r\log_2 M}{1+\alpha} = 1.64$ for $\alpha = 0.22$, which corresponds to the case that the transmission is successful with the first attempt. The $\tilde{E}_{\mathrm{t}}(\eta_{\mathrm{s}})$ curve contains two special points: the point $(\hat{\eta}_{\mathrm{s}}, \hat{E}_{\mathrm{t}})$ corresponds to the optimum solution obtained by minimizing E_{t} from Section III; the point $(\check{\eta}_{\mathrm{s}}, \check{E}_{\mathrm{t}})$ corresponds to the optimum solution of minimizing E_{m} obtained from Section IV.

The EE-SE tradeoff for a type-I ARQ system is given in Theorem 1.

Theorem 1: For a given η_{s} in a type-I ARQ system, the minimum E_{t} can be computed by using the parameters in Lemma 2. The resulting $\tilde{E}_{\mathrm{t}}(\eta_{\mathrm{s}})$ curve is quasiconvex in η_{s}.

Proof: The proof of the theorem is in Appendix M. ■

Based on Theorem 1, we know that $(\hat{\eta}_{\mathrm{s}}, \hat{E}_{\mathrm{t}})$ corresponds to the point with the global minimum E_{t}, and its corresponding $\hat{\eta}_{\mathrm{s}}$ divides the curve into two regions: Region 1 with $\eta_{\mathrm{s}} < \hat{\eta}_{\mathrm{s}}$ (with a negative slope) and Region 2 with $\eta_{\mathrm{s}} \geq \hat{\eta}_{\mathrm{s}}$ (with a positive slope). Furthermore, minimizing E_{m} guarantees that the operation point $(\check{\eta}_{\mathrm{s}}, \check{E}_{\mathrm{t}})$ falls in Region 2 of the $\tilde{E}_{\mathrm{t}}(\eta_{\mathrm{s}})$ curve, which further divides Region 2 into two subregions: $\eta_{\mathrm{s}} < \check{\eta}_{\mathrm{s}}$ (denoted as region 2L) and $\eta_{\mathrm{s}} \geq \check{\eta}_{\mathrm{s}}$ (denoted as region 2R).

Now we are ready to solve our original optimization problem with the practical constraint $\eta_{\mathrm{s}} \geq \eta_{\mathrm{th}}$ by noting which

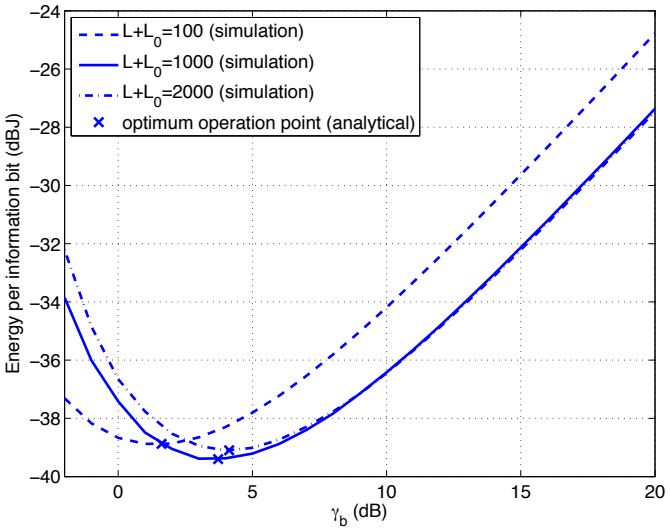

Fig. 5. Energy per information bit E_{t} v.s. γ_{b} at the receiver.

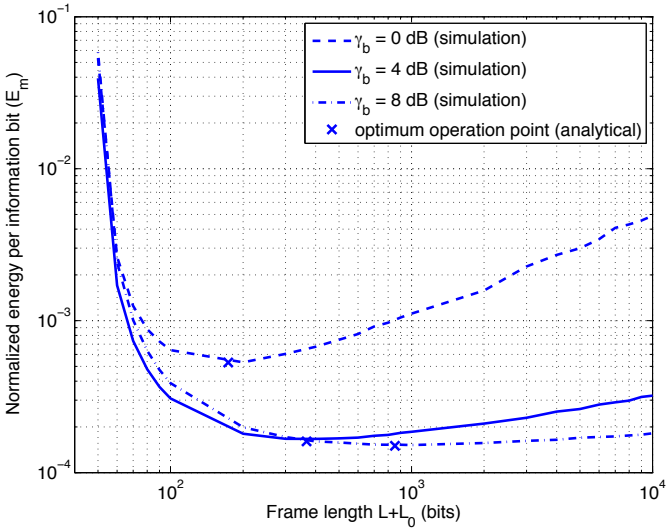

Fig. 6. Normalized energy per information bit E_{m} v.s. number of bits per frame $L + L_0$.

region the threshold η_{th} falls in. The solution to the original problem (18) is stated as follows.

Corollary 7: Denote $\hat{\eta}_{\mathrm{s}}$ as the spectral efficiency corresponding to the global minimum E_{t} as obtained in Propositions 1 and 2. If $\eta_{\mathrm{th}} < \hat{\eta}_{\mathrm{s}}$, then the optimum solution to (18) coincides with the results in Propositions 1 and 2. If $\eta_{\mathrm{th}} \geq \hat{\eta}_{\mathrm{s}}$, then the optimum solution can be calculated using Lemma 2.

Proof: The results can be directly obtained by using the E_{t}–η_{s} tradeoff relation described in Theorem 1. ■

Corollary 7 provides a generalized optimum system design for type-I ARQ systems by considering both EE and SE. The results from Sections III and IV are special cases of Corollary 7. Given the two regions on the $\tilde{E}_{\mathrm{t}}(\eta_{\mathrm{s}})$ curve, none of the points in Region 1 is optimum with respect to (18). Consequently, no practical systems should operate in Region 1. In Region 2, E_{t} is a strictly increasing function in η_{s}, which means the EE has to be improved at the cost of SE or vice versa. Each point in Region 2 of the $\tilde{E}_{\mathrm{t}}(\eta_{\mathrm{s}})$ curve corresponds to one possible EE-SE tradeoff, allowing flexible designs according to the requirement of the specific applications. In general, the E_{t}–η_{s} slope is relatively small in Region 2L. Therefore, we can achieve a relatively large improvement in η_{s} with only a small cost in E_{t} in Region 2L. In contrast, Region 2R has a large slope, which means that a small improvement in SE is achieved as a large cost of the EE. Therefore, Region 2L is the most desirable operation region for the EE-SE tradeoff.

VI. Numerical Results

An ARQ system was simulated in the PHY and MAC layers, including channel coding and decoding, baseband modulation and demodulation, protocol overhead, and retransmissions, etc. Most of the simulation parameters followed those in [2] with $\mu = 3.5$, $\beta = 310.014$ mw, $N_0/2 = -174$ dBm/Hz, G_1 =30 dB, $\kappa = 3.5$, and M_{l} = 40 dB. The rest of the parameters are $L_0 = 48$, $\alpha = 0.22$, and a fixed bit rate $R_{\mathrm{b}} = 300$ kbps. The channel code used in the simulation was a rate $r = \frac{1}{2}$ convolutional code with generator polynomial $[5, 7]_8$ and constraint length of 3.

Figure 5 shows E_{t} as a function of γ_{b} with various values of $L + L_0$. The communication distance was $d = 100$ m. It can be seen from the figure that E_{t} is a convex function in γ_{b}. The optimum values of $\hat{\gamma}_{\mathrm{b}}$ for different L calculated from (13) are marked on the figure as "x", which match nicely with the simulation results. If $\gamma_{\mathrm{b}} < \hat{\gamma}_{\mathrm{b}}$, then the FER is so high that the total energy consumption is dominated by retransmissions. In this case, we can *reduce* the total energy consumption by *increasing* γ_{b}. For example, for $L + L_0 = 1,000$ bits, increasing γ_{b} from -2 dB to 5 dB can save 5.3 dB energy per bit. If $\gamma_{\mathrm{b}} > \hat{\gamma}_{\mathrm{b}}$, then E_{t} increases almost linearly with γ_{b} because the FER is low enough and the effect of retransmission is negligible. The result demonstrates that a higher E_{b}/N_0 does not necessarily translate into better performance in energy efficiency. Significant energy saving can be achieved by carefully choosing the operation point.

In Fig. 6, the normalized energy per information bit E_{m} is plotted as a function of $L + L_0$ under several values of γ_{b}. Again, the communication distance was $d = 100$ m. As expected, E_{m} is convex in $\log(L + L_0)$, as shown by the simulation curves. The optimum values $\check{L}$ calculated from (17) are marked as "x" in the figure. Excellent agreement is observed between the analytical optimum operation points and the simulation results. When γ_{b} is small, increasing L passing its optimum operation point leads to a fast performance degradation. On the other hand, when γ_{b} is large, for example, $\gamma_{\mathrm{b}} = 8$ dB, increasing L passing its optimum operation point has a much smaller impact, because the FER only degrades slightly with L at high γ_{b}. Therefore, the EE performance of a system operating at low γ_{b} is more sensitive to the frame length.

In Figures 7 and 8, we compare the E_{t} and η_{s} obtained from the three different optimum designs: minimizing E_{t}, minimizing E_{m}, and minimizing E_{t} with the constraint $\eta_{\mathrm{s}} \geq \eta_{\mathrm{th}}$. The modulation scheme was 16QAM and the communication

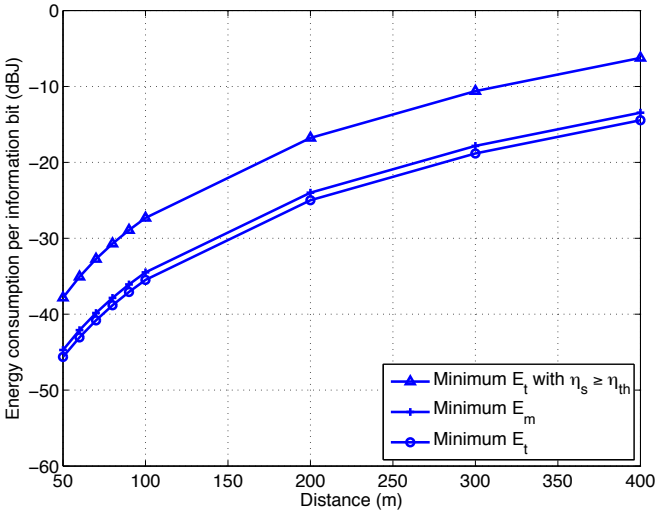

Fig. 7. Energy per information bit required by the three optimum designs.

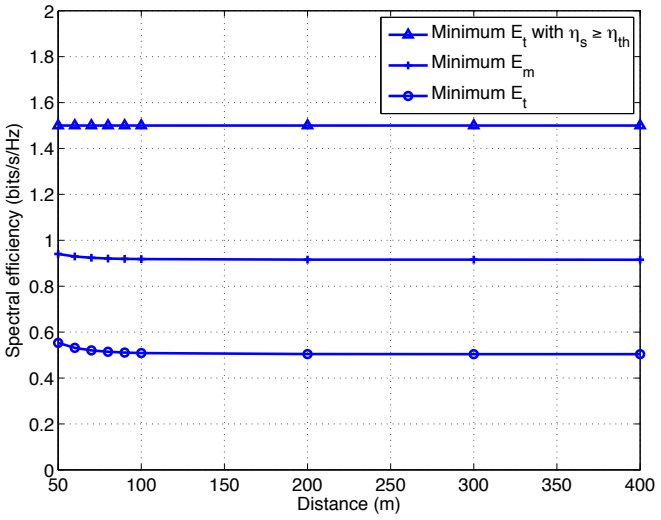

Fig. 8. Spectral efficiency achieved by the three optimum designs.

distance varied from 50 m to 400 m. For minimizing $E_{\rm t}$ with the SE constraint, we set $\eta_{\rm th} = 1.5$ bps/Hz. It can be seen from the figures that, although the design from minimizing $E_{\rm t}$ achieves the lowest energy consumption, the corresponding SE is also very low. In contrast, the design from minimizing $E_{\rm m}$ can almost double the spectral efficiency with very small increase in energy consumption. At $d = 100$ m, the SE of the minimum $E_{\rm m}$ scheme outperforms the minimum $E_{\rm t}$ one by 80%, with only a 0.9 dB increase in energy consumption. For the optimum design with the SE constraint, it is possible to achieve a very high SE at the cost of increased energy consumption. At $d = 100$ m, increasing the SE from 0.9 bps/Hz to 1.5 bps/Hz results in a 7 dB increase in energy consumption. Other EE-SE tradeoffs can be obtained by setting different thresholds in the constrained optimization scheme.

VII. Conclusions

The energy efficient and spectral efficient designs have been studied for type-I ARQ systems operating in quasi-static Rayleigh fading channels. A new log-domain threshold approximation method has been proposed to facilitate the system design. The optimum transmission energy and frame length for various design criteria have been identified, and most are in closed-form expressions. With insights gained through the design results, the fundamental EE-SE tradeoff in type-I ARQ systems has been theoretically identified. It has been shown that the minimum $E_{\rm t}$ is quasiconvex in $\eta_{\rm s}$, and the optimum operation points are always in the positive slope region of the $E_{\rm t}$–$\eta_{\rm s}$ curve. From the analytical and simulation results, we have the following observations: 1) The total energy per information bit could be *reduced* by *increasing* the energy used in one transmission attempt if the system operates in the negative slope region of the $E_{\rm t}$–$\eta_{\rm s}$ curve; 2) systems operating at higher $E_{\rm b}/N_0$ are less sensitive to the frame length change; 3) optimizing with respect to $E_{\rm m}$ instead of $E_{\rm t}$ can almost double the spectral efficiency with less than 1 dB more cost in $E_{\rm t}$; 4) increasing the SE beyond the value corresponding to the minimum $E_{\rm m}$ might lead to significant cost in $E_{\rm t}$.

Appendix

A. Proof of Lemma 1

Consider $0 < x_1 < x_2$ and $\varepsilon \in [0,1]$. Define $\theta_1 = \varepsilon f(x_1)g(x_1) + (1-\varepsilon)f(x_2)g(x_2)$, and $\theta_2 = f(\varepsilon x_1 + (1-\varepsilon)x_2)g(\varepsilon x_1 + (1-\varepsilon)x_2)$. It is sufficient to prove that $\theta_1 \le \theta_2$.

Since $f(x)$ and $g(x)$ are convex, we have $\theta_2 \ge \theta_3$ with θ_3 defined as

$$\theta_3 = [\varepsilon f(x_1) + (1-\varepsilon)f(x_2)][\varepsilon g(x_1) + (1-\varepsilon)g(x_2)] \quad (25)$$

Since $\theta_1 = \theta_1(1-\varepsilon+\varepsilon)$, the term θ_1 can be alternatively represented as

$$\begin{aligned}\theta_1 \;=\; & \varepsilon^2 f(x_1)g(x_1) + (1-\varepsilon)^2 f(x_2)g(x_2) + \\ & \varepsilon(1-\varepsilon)\left[f(x_1)g(x_1) + f(x_2)g(x_2)\right] \end{aligned} \quad (26)$$

From (25) and (26), we have

$$\frac{\theta_3 - \theta_1}{\varepsilon(1-\varepsilon)} = [f(x_1) - f(x_2)][g(x_2) - g(x_1)] \ge 0. \quad (27)$$

Therefore $\theta_2 \ge \theta_3 \ge \theta_1$, and this completes the proof.

B. Proof of Corollary 1

We first prove that Λ is convex in $\gamma_{\rm b}$. The first derivative of Λ with respect to $\gamma_{\rm b}$ is

$$\frac{\partial \Lambda}{\partial \gamma_{\rm b}} = -\frac{\gamma_\omega}{\gamma_{\rm b}^2} \exp\left(\frac{\gamma_\omega}{\gamma_{\rm b}}\right) \le 0. \quad (28)$$

Denote $\mathrm{FER}'(\gamma_{\rm b}) = \frac{\partial \mathrm{FER}}{\partial \gamma_{\rm b}}$ and $\mathrm{FER}''(\gamma_{\rm b}) = \frac{\partial^2 \mathrm{FER}}{\partial \gamma_{\rm b}^2}$. The second derivative of Λ with respect to $\gamma_{\rm b}$ can be expressed as

$$\frac{\partial^2 \Lambda}{\partial \gamma_{\rm b}^2} = \frac{\mathrm{FER}''(\gamma_{\rm b})(1-\mathrm{FER}) + 2\left[\mathrm{FER}'(\gamma_{\rm b})\right]^2}{\left[1-\mathrm{FER}\right]^3}. \quad (29)$$

From (12), we have

$$\mathrm{FER}'(\gamma_\mathrm{b}) = -\frac{\gamma_\omega}{\gamma_\mathrm{b}^2}\exp\left(-\frac{\gamma_\omega}{\gamma_\mathrm{b}}\right), \quad (30a)$$

$$\mathrm{FER}''(\gamma_\mathrm{b}) = \frac{\gamma_\omega}{\gamma_\mathrm{b}^3}\left(2-\frac{\gamma_\omega}{\gamma_\mathrm{b}}\right)\exp\left(-\frac{\gamma_\omega}{\gamma_\mathrm{b}}\right). \quad (30b)$$

Substituting the above results into (29) and simplifying lead to

$$\frac{\partial^2\Lambda}{\partial\gamma_\mathrm{b}^2} = \frac{\gamma_\omega}{\gamma_\mathrm{b}^3}\left(2+\frac{\gamma_\omega}{\gamma_\mathrm{b}}\right)\exp\left(\frac{\gamma_\omega}{\gamma_\mathrm{b}}\right) \geq 0. \quad (31)$$

Therefore Λ is decreasing and convexity function in γ_b. It is straightforward to show that E_0 is a linear increasing function in γ_b. Based on Theorem 1, $E_\mathrm{t} = \Lambda E_0$ is convex in γ_b.

C. Proof of Proposition 1

Since E_t is convex in γ_b, the optimum γ_b that minimize E_t can be obtained by solving $\frac{\partial E_\mathrm{t}}{\partial\gamma_\mathrm{b}} = 0$, which yields

$$\gamma_\mathrm{b}^2 - \gamma_\omega\gamma_\mathrm{b} - \gamma_\omega\frac{B}{A}\frac{L}{L+L_0} = 0. \quad (32)$$

The result in (13) can be obtained by solving (32).

D. Proof of Corollary 2

From (6), we have

$$\frac{\partial^2\Lambda}{\partial\xi^2} = \left(\frac{k_{_M}}{\gamma_\mathrm{b}}\right)^2\exp\left(-\frac{k_{_M}\xi}{\gamma_\mathrm{b}}\right) \geq 0. \quad (33)$$

Therefore Λ is convex in ξ. It is also straightforward to show that Λ is an increasing function in ξ.

From (5), we have $E_0 = A\gamma_\mathrm{b}\left(1+\frac{L_0}{e^\xi - L_0}\right) + B$, and

$$\frac{\partial^2 E_0}{\xi^2} = A\gamma_\mathrm{b}L_0\frac{e^\xi(e^\xi+L_0)}{(e^\xi-L_0)^3} \geq 0. \quad (34)$$

Therefore E_0 is convex in ξ. In addition, E_0 is a decreasing function in ξ. The convexity of E_t is then proved by using Theorem 1.

E. Proof of Proposition 2

The optimum L is obtained by solving $\frac{\partial E_\mathrm{n}}{\partial\xi} = 0$, which yields

$$k_{_M}(A\gamma_\mathrm{b}+B)L^2 + A\gamma_\mathrm{b}L_0\left(k_{_M}-\gamma_\mathrm{b}\right)L - A\gamma_\mathrm{b}^2L_0^2 = 0. \quad (35)$$

The result in (15) can be obtained by solving (35).

F. Proof of Corollary 3

Assume the values after the i-th iteration is $\boldsymbol{\pi}^{(i)} = [\gamma_\mathrm{b}^{(i)}, L^{(i)}]^T$. During the $(i+1)$-th iteration, we can first calculate $\gamma_\mathrm{b}^{(i+1)}$ by using (13) and $L^{(i)}$. Based on Proposition 1, $E_\mathrm{t}(\gamma_\mathrm{b}^{(i+1)}, L^{(i)}) \leq E_\mathrm{t}(\gamma_\mathrm{b}^{(i)}, L^{(i)})$. Then $L^{(i+1)}$ can be calculated by using (15) and $\gamma_\mathrm{b}^{(i+1)}$. Based on Proposition 2, $E_\mathrm{t}(\gamma_\mathrm{b}^{(i+1)}, L^{(i+1)}) \leq E_\mathrm{t}(\gamma_\mathrm{b}^{(i+1)}, L^{(i)})$. If $\boldsymbol{\pi}^{(i)} \neq \hat{\boldsymbol{\pi}}$, then $E_\mathrm{t}(\gamma_\mathrm{b}^{(i+1)}, L^{(i+1)}) < E_\mathrm{t}(\gamma_\mathrm{b}^{(i)}, L^{(i)})$, i.e., the value of E_t will decrease after each iteration, and $\boldsymbol{\pi}^{(i)}$ is converging to its globally optimum value given that there is a minimum E_t. If $\boldsymbol{\pi}^{(i)} = \hat{\boldsymbol{\pi}}$, then $E_\mathrm{t}(\gamma_\mathrm{b}^{(i+1)}, L^{(i+1)}) = E_\mathrm{t}(\gamma_\mathrm{b}^{(i)}, L^{(i)})$, and the iteration converges.

G. Proof of Corollary 4

The first derivative of Δ_1 with respect to γ_b is

$$\frac{\partial\Delta_1}{\partial\gamma_\mathrm{b}} = -\frac{2\gamma_\omega}{\gamma_\mathrm{b}^2}\exp\left(\frac{2\gamma_\omega}{\gamma_\mathrm{b}}\right) \leq 0. \quad (36)$$

Therefore Δ_1 is a decreasing function in γ_b.

The second derivative of Δ_1 with respect to γ_b is

$$\frac{\partial^2\Delta_1}{\partial\gamma_\mathrm{b}^2} = \frac{2\mathrm{FER}''(\gamma_\mathrm{b})(1-\mathrm{FER}) + 6[\mathrm{FER}'(\gamma_\mathrm{b})^2]}{(1-\mathrm{FER})^4}. \quad (37)$$

Substituting (30) into (37) and simplifying lead to

$$\frac{\partial^2\Delta_1}{\partial\gamma_\mathrm{b}^2} = \frac{4\gamma_\omega}{\gamma_\mathrm{b}^4}(\gamma_\mathrm{b}+\gamma_\omega)\exp\left(\frac{2\gamma_\omega}{\gamma_\mathrm{b}}\right) \geq 0. \quad (38)$$

Therefore Δ_1 is convex in γ_b.

It is straightforward that Δ_2 is a linear increasing function in γ_b. Based on Theorem 1, $E_\mathrm{m} = \Delta_1\Delta_2$ is convex in γ_b.

H. Proof of Proposition 3

Since E_m is convex in γ_b, the optimum γ_b that minimize E_m can be obtained by solving $\frac{\partial E_\mathrm{m}}{\partial\gamma_\mathrm{b}} = 0$, which yields

$$\frac{\partial\Delta_1}{\partial\gamma_\mathrm{b}}\Delta_2 + \frac{\partial\Delta_2}{\partial\gamma_\mathrm{b}}\Delta_1 = 0. \quad (39)$$

Since $\frac{\partial\Delta_2}{\partial\gamma_\mathrm{b}} = \left(\frac{L+L_0}{L}\right)^2 AC$. Substituting (36) into (39) leads to

$$\gamma_\mathrm{b}^2 - 2\gamma_\omega\gamma_\mathrm{b} - 2\gamma_\omega\frac{B}{A}\frac{L}{L+L_0} = 0. \quad (40)$$

The result in (16) can be obtained by solving (40).

I. Proof of Corollary 5

From the definition of Δ_1, we have

$$\frac{\partial^2\Delta_1}{\partial\xi^2} = \frac{4k_{_M}^2}{\gamma_\mathrm{b}^2}\exp\left(\frac{2\gamma_\omega}{\gamma_\mathrm{b}}\right) \geq 0. \quad (41)$$

Therefore Δ_1 is convex in ξ. It is also straightforward to show that Δ_1 is an increasing function in ξ.

In addition, Δ_2 can be alternatively expressed as

$$\Delta_2 = \left(1+\frac{L_0}{e^\xi-L_0}\right)\left[A\gamma_\mathrm{b}\left(1+\frac{L_0}{e^\xi-L_0}\right)+B\right]\frac{1}{\eta_{_M}},$$

and

$$\frac{\partial^2\Delta_2}{\partial\xi^2} = L_0\frac{e^\xi\left[2\gamma_\mathrm{b}Ae^\xi(2e^\xi+L_0-1)+B(e^{2\xi}-L_0^2)\right]}{\eta_{_M}(e^\xi-L_0)^4} \geq 0.$$

Therefore Δ_2 is convex in ξ. In addition, Δ_2 is a decreasing function in ξ. The convexity of E_m with respect to ξ is then proved by using Theorem 1.

J. Proof of Proposition 4

The optimum L is obtained by solving $\frac{\partial E_{\mathrm{m}}}{\partial \xi} = 0$, which yields

$$\frac{\partial \Delta_1}{\partial \xi}\Delta_2 + \frac{\partial \Delta_2}{\partial \xi}\Delta_1 = 0. \tag{42}$$

Since

$$\frac{\partial \Delta_1}{\partial \xi} = \frac{2k_{_M}}{\gamma_{\mathrm{b}}}\exp\left(\frac{2\gamma_\omega}{\gamma_{\mathrm{b}}}\right), \tag{43a}$$

$$\frac{\partial \Delta_2}{\partial \xi} = -\frac{L_0 e^{\xi}}{\eta_{_M}(e^{\xi}-L_0)^2}\left(\frac{2A\gamma_{\mathrm{b}}e^{\xi}}{e^{\xi}-L_0}+B\right). \tag{43b}$$

Substituting the above results into (42) leads to

$$2k_{_M}(A\gamma_{\mathrm{b}}+B)L^2+\gamma_{\mathrm{b}}L_0(2Ak_{_M}-2A\gamma_{\mathrm{b}}-B)L-2A\gamma_{\mathrm{b}}^2L_0^2=0.$$

The result in (17) can be obtained by solving the above equation.

K. Proof of Lemma 2

Substituting (21) into the equation $\partial\psi(\gamma_{\mathrm{b}},L)/\partial\gamma_{\mathrm{b}} = 0$ yields

$$\lambda\eta_{\mathrm{th}}\frac{\gamma_\omega}{\gamma_{\mathrm{b}}^2} = \frac{\eta_{_M}}{\eta_{\mathrm{th}}}\left(\frac{\gamma_\omega}{\gamma_{\mathrm{b}}^2}\frac{L}{L+L_0}B - A + \frac{\gamma_\omega}{\gamma_{\mathrm{b}}}A\right). \tag{44}$$

Similarly, combining (21) with $\partial\psi(\gamma_{\mathrm{b}},L)/\partial L = 0$, we have

$$\lambda\eta_{\mathrm{th}}\frac{L_0\gamma_{\mathrm{b}}-k_{_M}L}{L\gamma_{\mathrm{b}}} = \frac{L\eta_{_M}}{\eta_{\mathrm{th}}}\left(\gamma_{\mathrm{b}}A\frac{L_0}{L^2}-\frac{k_{_M}}{L}A-\frac{k_{_M}}{\gamma_{\mathrm{b}}}\frac{B}{L+L_0}\right). \tag{45}$$

The Lagrangian multiplier λ can be removed by dividing (44) by (45) and the result is

$$\frac{\gamma_\omega}{\gamma_{\mathrm{b}}}L^2\left(\gamma_{\mathrm{b}}A\frac{L_0}{L^2}-\frac{k_{_M}}{L}A-\frac{k_{_M}}{\gamma_{\mathrm{b}}}\frac{1}{L+L_0}B\right) = (L_0\gamma_{\mathrm{b}}-k_{_M}L)\left(\frac{\gamma_\omega}{\gamma_{\mathrm{b}}^2}\frac{L}{L+L_0}B - A + \frac{\gamma_\omega}{\gamma_{\mathrm{b}}}A\right).$$

Rearranging the terms, we obtain a second order linear equation in γ_{b}

$$\gamma_{\mathrm{b}}^2 - k_{_M}\frac{L}{L_0}\gamma_{\mathrm{b}} - \gamma_\omega\frac{B}{A}\frac{L}{L+L_0} = 0. \tag{46}$$

Solving (46) yields the desired solution (23).

To solve for optimum L, combining (11) and (21) yields

$$\frac{k_{_M}}{\gamma_{\mathrm{b}}}\log(L+L_0)+\frac{b_{_M}}{\gamma_{\mathrm{b}}} = \log\frac{L}{L+L_0}+\log\frac{\eta_{_M}}{\eta_{\mathrm{th}}}. \tag{47}$$

which is simplified to (24).

L. Proof of Corollary 6

Eqn. (23) can be alternatively written as

$$\tilde{\gamma}_{\mathrm{b}} = \frac{1}{2}\left(k_{_M}\frac{\tilde{L}}{L_0}+\sqrt{\left(k_{_M}\frac{\tilde{L}}{L_0}\right)^2+4\gamma_\omega\frac{B}{A}\frac{1}{1+L_0/\tilde{L}}}\right). \tag{48}$$

Since γ_ω is a strictly increasing function in $\tilde{L}$, it is straightforward that the optimum γ_{b} strictly increases with $\tilde{L}$.

Performing differentiation of η_{s} in (8) with respect to γ_{b}, we have $\frac{\partial\eta_{\mathrm{s}}}{\partial\gamma_{\mathrm{b}}} = \eta_{\mathrm{s}}\frac{\gamma_\omega}{\gamma_{\mathrm{b}}^2} > 0$, thus statement 2) is proved.

Performing differentiation of η_{s} in (8) with respect to L, we have

$$\frac{\partial\eta_{\mathrm{s}}}{\partial L} = \frac{\eta_{_M}(1-\mathrm{FER})}{(L+L_0)^2}\left(L_0-\frac{k_{_M}}{\gamma_{\mathrm{b}}}L\right). \tag{49}$$

Thus statement 3) can be proved by showing $L_0 > \frac{k_{_M}}{\gamma_{\mathrm{b}}}\tilde{L}$. From (23), we have

$$\frac{k_{_M}}{\gamma_{\mathrm{b}}}\tilde{L} = L_0\cdot 2k_{_M}/\left(k_{_M}+\sqrt{k_{_M}^2+4\gamma_\omega\frac{B}{A}\frac{L_0^2}{L(L+L_0)}}\right) < L_0\cdot 2k_{_M}/(k_{_M}+k_{_M}) = L_0. \tag{50}$$

Thus statement 3) is true.

M. Proof of Theorem 1

The quasiconvexity can be proved by showing that 1) $\tilde{E}_{\mathrm{t}}(\eta_{\mathrm{s}})$ is continuous in η_{s}; 2) $\tilde{E}_{\mathrm{t}}(\eta_{\mathrm{s}})$ is a strictly decreasing function in η_{s} for $\eta_{\mathrm{s}} < \hat{\eta}_{\mathrm{s}}$; and 3) $\tilde{E}_{\mathrm{t}}(\eta_{\mathrm{s}})$ is a strictly increasing function in η_{s} for $\eta_{\mathrm{s}} > \hat{\eta}_{\mathrm{s}}$.

The continuity of $\tilde{E}_{\mathrm{t}}(\eta_{\mathrm{s}})$ can be directly established because (7), (8), (23), and (24) are continuous functions.

Consider $\eta_{\mathrm{s}1} < \eta_{\mathrm{s}2} < \hat{\eta}_{\mathrm{s}}$. Given $\eta_{\mathrm{s}i}$, we can calculate the values of $[\tilde{\gamma}_{\mathrm{b}i}, \tilde{L}_i]$ that minimize E_{t} from Lemma 2, for $i = 1, 2$. Denote the corresponding minimum E_{t} as $\tilde{E}_{\mathrm{t}}(\eta_{\mathrm{s}i})$, for $i = 1, 2$. Based on the results in Corollary 6, we have

$$\tilde{\gamma}_{\mathrm{b}1} < \tilde{\gamma}_{\mathrm{b}2} < \hat{\gamma}_{\mathrm{b}}, \text{ and } \tilde{L}_2 < \tilde{L}_1 < \hat{L}, \tag{51}$$

where $\hat{\gamma}_{\mathrm{b}}$ and $\hat{L}$ achieve the globally minimum E_{t} with the SE $\eta_{\mathrm{s}} = \hat{\eta}_{\mathrm{s}}$.

The inequality in (51) can be easily proved through contradiction. Assume $\tilde{\gamma}_{\mathrm{b}1} \geq \tilde{\gamma}_{\mathrm{b}2}$. Then based on statement 1) in Corollary 6, $\tilde{L}_1 \geq \tilde{L}_2$. Based on statements 2) and 3) in corollary 6, $\eta_{\mathrm{s}1} \geq \eta_{\mathrm{s}2}$, and this contradicts with $\eta_{\mathrm{s}1} < \eta_{\mathrm{s}2}$. Therefore, $\tilde{\gamma}_{\mathrm{b}1} < \tilde{\gamma}_{\mathrm{b}2}$. All the inequalities in (51) can be proved in a similar manner.

From Corollaries 1 and 2, E_{t} is convex in γ_{b} and $\xi = \log(L+L_0)$, with the zero-slope point being $\hat{\gamma}_{\mathrm{b}}$ and $\log(\hat{L}+L_0)$. Consequently, E_{t} is a strictly decreasing function in γ_{b} for $\gamma_{\mathrm{b}} < \hat{\gamma}_{\mathrm{b}}$, and it is a strictly decreasing function in L for $L < \hat{L}$. Therefore, from (51), $\tilde{E}_{\mathrm{t}}(\eta_{\mathrm{s}1}) > \tilde{E}_{\mathrm{t}}(\eta_{\mathrm{s}2})$, or E_{t} is a strictly decreasing function in η_{s} for $\eta_{\mathrm{s}} < \hat{\eta}_{\mathrm{s}}$.

Similarly, we can prove that $\tilde{E}_{\mathrm{t}}(\eta_{\mathrm{s}})$ is a strictly increasing function in η_{s} for $\eta_{\mathrm{s}} > \hat{\eta}_{\mathrm{s}}$. This completes the proof.

REFERENCES

[1] G. Y. Li, Z. Xu, C. Xiong, C. Yang, S. Zhang, Y. Chen, and S. Xu, "Energy-efficient wireless communications: tutorials, survey, and open issues," *IEEE Trans. Wireless Communications*, vol. 18, pp. 28 - 35, 2011.

[2] S. Cui, A. J. Goldsmith, and A. Bahai, "Energy-constrained modulation optimization," *IEEE Trans. Wireless Commun.*, vol. 4, pp. 2349 - 2360, Sept. 2005.

[3] F. M. Costa and H. Ochiai, "Energy-efficient physical layer design for wireless sensor network links," *IEEE Int. Conf. Commun. (ICC)*, Kyoto, Japan, Jun. 2011. pp. 1-5.

[4] W. Ye, J. Heidemann, and D. Estrin, "Medium access control with coordinated adaptive sleeping for wireless sensor networks," *IEEE/ACM Trans. Netw.*, vol. 12, pp.493 - 506, June 2004.

[5] A. E. Gamal, C. Nair, B. Prabhakar, E. Uysal-Biyikoglu, and S. Zahedi, "Energy-efficiency scheduling of packet transmissions over wireless networks," *IEEE INFOCOM 2002*, vol. 3, June 2002. pp. 1773 - 1782.

[6] W. Su, S. Lee, D. A. Pados, and J. D. Matyjas, "Optimal power assignment for minimizing the average total transmission power in hybrid-ARQ Rayleigh fading links," *IEEE Trans. Commun.*, vol. 59, no. 7, pp.1867 - 1877, July 2011.
[7] T. Chaitanya and E. Larsson, "Outage-optimal power allocation for hybrid ARQ with incremental redundancy," *IEEE Trans. Wireless Commun.*, vol. 10, pp.2069 - 2074, Jul. 2011.
[8] S. Verdu, "Spectral efficiency in the wideband regime," *IEEE Trans. Inf. Theory*, vol. 48, pp. 1319 - 1343, June 2002.
[9] C. Xiong, G. Y. Li, S. Zhang, Y. Chen, and S. Xu, "Energy- and spectral-efficiency tradeoff in downlink OFDMA networks," *IEEE Trans. Wireless Commun.*, vol. 10, pp.3874 - 3886, Nov. 2011.
[10] Y. Chen, S. Zhang, S. Xu, and G. Y. Li, "Fundamental tradeoffs on green wireless networks," *IEEE Commun. Mag.*, vol. 49, pp.30-37, June 2011.
[11] D. Tuninetti, "On the benefits of partial channel state information for repetition protocols in block fading channels," *IEEE Trans. Inf. Theory*, vol. 57, pp.5036 - 5053, Aug. 2011.
[12] G. Wang, J. Wu, and Y. R. Zheng, "Cross-layer design of energy efficient coded ARQ systems," *IEEE Global Telecommun. Conf. (Globecom)*, Anaheim, CA, Dec. 2012. pp.1-5.
[13] K. Nguyen, L. Rasmussen, A. Guillen i Fabregas, and N. Letzepis, "MIMO ARQ with multibit feedback: outage analysis," *IEEE Trans. Information Theory*, vol. 58, pp.765 - 779, Feb. 2012.
[14] J. Cioffi, *Digital Communications.* Stanford Univ. Press, 2001.
[15] I. Chatzigeorgiou, I. J. Wassell, and R. Carrasco, "On the frame error rate of transmission schemes on quasi-static fading channels," *42nd Annual Conf. Information Sciences Systems (CISS)*, Mar. 2008. pp. 577 - 581.
[16] E. Biglieri, G. Caire, and G. Taricco, "Limiting performance of block-fading channels with multiple antennas," *IEEE Trans. Information Theory*, vol. 47, no. 4, pp. 1273 - 1289, May 2001.
[17] R. Knopp and P. A. Humblet, "On coding for block fading channels," *IEEE Trans. Inf. Theory*, vol. 46, no. 1, pp. 189 - 205, Jan. 2000.
[18] C. Schlegel and L. Perez, "On error bounds and Turbo-codes," *IEEE Commun. Lett.*, vol. 3, no. 7, pp. 205 - 207, July 1999.

Jingxian Wu (S'02-M'06) received the B.S. (EE) degree from the Beijing University of Aeronautics and Astronautics, Beijing, China, in 1998, the M.S. (EE) degree from Tsinghua University, Beijing, China, in 2001, and the Ph.D. (EE) degree from the University of Missouri at Columbia, MO, USA, in 2005. He is currently an Assistant Professor with the Department of Electrical Engineering, University of Arkansas, Fayetteville. His research interests mainly focus on wireless communications and wireless networks, including ultra-low power communications, energy efficient communications, cognitive radio, and cross-layer optimization, etc. He served as a Cochair for the 2012 Wireless Communication Symposium of the IEEE International Conference on Communication, and a Cochair for the 2009 Wireless Communication Symposium of the IEEE Global Telecommunications Conference. He served as an Associate Editor of the IEEE TRANSACTIONS ON VEHICULAR TECHNOLOGY from 2007 to 2011, and is now an Editor of the IEEE TRANSACTIONS ON WIRELESS COMMUNICATIONS.

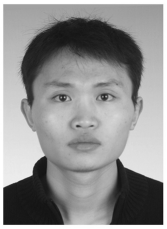

Gang Wang received the B.S. degree from the Northwestern Polytechnical University, Xi′an, China, in 2005, and the M.S. degree from Beihang University (with honor), Beijing, China, in 2008, both in electrical engineering. He then served as a system engineer in New Postcom Equipment Co., Ltd, in Beijing, from 2008 to 2010. He is currently a Ph.D. student at the Department of Electrical Engineering, University of Arkansas. His current research interests include energy-efficient system, convex optimization, cross-layer design, and wireless networks, etc. He is a member of Golden Key International Honor Society.

Yahong Rosa Zheng received the B.S. degree from the University of Electronic Science and Technology of China, Chengdu, China, in 1987, and the M.S. degree from Tsinghua University, Beijing, China, in 1989, both in electrical engineering. She received the Ph.D. degree from the Department of Systems and Computer Engineering, Carleton University, Ottawa, Canada, in 2002. She was an NSERC postdoctoral fellow from January 2003 to April 2005 at the University of Missouri-Columbia. Since 2005, she has been assistant then associate professor with the Department of Electrical and Computer Engineering at the Missouri University of Science and Technology (formerly the University of Missouri-Rolla). Her research interests include array signal processing, space-time adaptive processing, wireless communications, and wireless sensor networks. She has served as associate editor for IEEE Transactions on Wireless Communications 2006–2008 and is currently associate editor for IEEE Transactions on Vehicular Technology. She is the recipient of an NSF CAREER award in 2009.